



Scholars Research Library  
(<http://scholarsresearchlibrary.com/archive.html>)



ISSN : 2231- 3176  
CODEN (USA): JCMMDA

## Prediction on Binding affinity of some selected Coumarin and Anthraquinone Derivatives on Cysteine Rich C1 Domain of Kinase Suppressor of RAS-1(KSR-1) of MAPK signaling pathway

Dhananjayan Karthik

Department of Pharmacology, Amrita School of Pharmacy, AIMS Health Science Campus,  
Amrita Vishwa Vidyapeetham University, Kochi, Kerala, India.

### ABSTRACT

Kinase suppressor of Ras-1 (KSR1) is a conserved component of the Ras pathway that acts as a molecular scaffold to promote signal transmission from Raf-1 to MEK and MAPK. All KSR-1 proteins contain a conserved cysteine-rich C1 domain, and studies have implicated this domain in the regulation of KSR-1 sub cellular localization and function. In this study an evaluation on binding affinity of coumarin and anthraquinone derivatives on crystal structure of C1 domain of kinase suppressor of RAS was carried out using docking studies. Study showed the occupancy and importance of certain functional groups at the anthraquinone and coumarin nucleus responsible for its potential affinity in binding. These ligands can serve as a lead moiety in developing a targeted drug against the kinase suppressor of ras-1 to interrupt MAPK signaling in neoplasia.

**Keywords:** Kinase suppressor of Ras 1, Anthraquinone, Coumarin, AutoDock Vina, Docking, MAPK, Neoplasia.

### INTRODUCTION

The Ras pathway is an essential signal transduction cascade involved in cell proliferation, transformation, differentiation, and apoptosis [1]. KSR, a novel protein kinase required for RAS signal transduction. Kinase Suppressor of Ras (KSR) is a molecular scaffold that interacts with the core kinase components of the ERK cascade, Raf, MEK, and ERK and provides spatial and temporal regulation of Ras-dependent ERK cascade signaling. CK2 is a component of the KSR-1 scaffold complex that contributes to Raf kinase activation [2].

The KSR-1 scaffold translocate from the cytosol to the plasma membrane upon Ras activation and coordinates the assembly of a multi-protein complex that co-localizes MEK with its upstream activator Raf and downstream target ERK and thereby promotes signal transmission between the core kinase components of the ERK cascade [3, 4]. CK2 is a hetero-tetrameric serine/ threonine kinase composed of two regulatory,  $\beta$  and two catalytic subunits viz.,  $\alpha$  and/or  $\alpha'$  [5, 6]. KSR-1/CK2 interaction was confirmed through co-immune-precipitation assays. Moreover, binding of the CK2 subunits was found to be constitutive.

Members of the KSR family contain conserved protein domains (termed CA 1-5) and display remarkable overall sequence similarity to proteins of the Raf kinase family [7].

The conserved KSR domains include a 40 residue region unique to KSR proteins (CA1), a proline-rich region (CA2), a cysteine-rich C1 domain (CA3), a serine/threonine-rich region (CA4), and a putative kinase domain (CA5). Similar to the domain organization of Raf-1, the smaller conserved domains of KSR-1 are found in the N-terminal region, while the kinase-like domain occupies the C-terminal half of the protein. Unlike Raf-1, however, the kinase domain of KSR-1 appears to be non-functional, suggesting that KSR-1 does not promote Ras signaling by phosphorylating target molecules. C1 domains are defined as regions of approximately 50 amino acid residues that contain the motif  $HX_{10-12}CX_2CX_{11-19}CX_2CX_4HX_{2-4}CX_{5-9}C$  [8]. C1A and C1B are the two repeat C1 domains located within the same protein. C1 domains were initially identified as the phorbol ester and 1, 2-dialyglycerol binding moieties of the protein kinase C (PKC) family of serine/ threonine kinases [9]. **Figure 1** shows stereo ribbon diagram of C1 domain of KSR-1. Globular structure comprised of two  $\beta$ -sheets and a small  $\alpha$ -helix, with three cysteines and one histidine coordinating a single  $Zn^+$  ion at the end of each  $\beta$ -sheet was elucidated from the solution structure of the C1B domain of PKC $\alpha$  by NMR studies [10], and co-crystallization of PKC $\delta$ C1B domain with bound phorbol 13-acetate [11].

There is a ligand-binding cleft at the top of the domain which is composed of positively charged residues, surrounded by hydrophobic residues. Water molecules within the cleft are displaced due to lipid binding and generate a continuous hydrophobic surface that facilitates tight association with membrane. C1 domains have been classified into two types based on structure and function, the typical C1 domain that binds phorbol ester/1, 2-diaclyglycerol (DAG) and the atypical C1 domain that does not [12]

Research involved in targeting scaffold protein is vast. Antibody against KSR 1 and KSR 2 are available, but they are of only research purpose. RGS19 inhibits Ras signaling through Nm23H1/2-mediated phosphorylation of the kinase suppressor of Ras [13]

There are some specific antibodies that have affinity towards ksr, like hKSR-2 inhibits MEKK3-activated MAP kinase and NF-kappa-B pathways in inflammation [14].

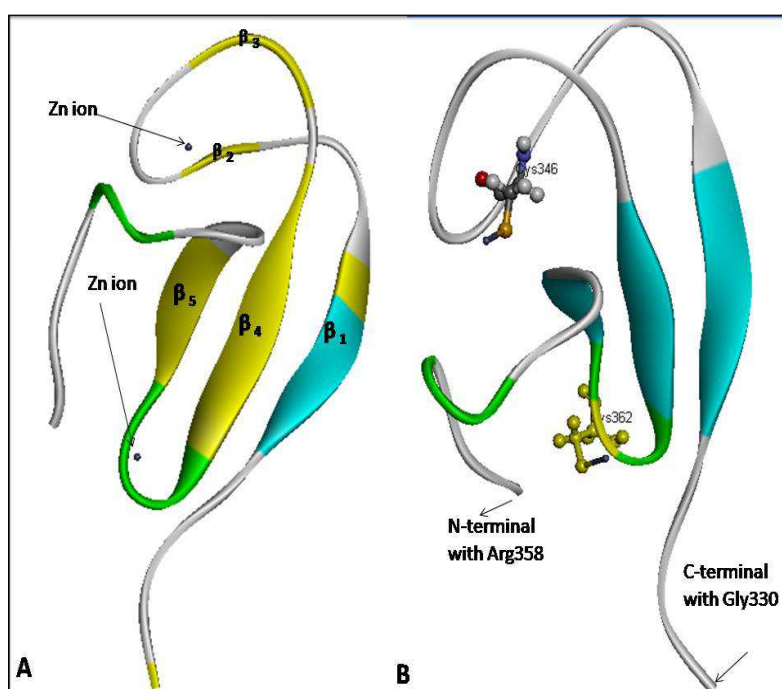


**Figure 1:** Image showing the stereo ribbon diagram of KSR-1 C1 domain (RCSB PDB CODE: 1KBE) generated using Accelrys Discovery studio 3.1 (A) Beta strands ( $\beta_1$ ,  $\beta_2$ ,  $\beta_3$ ,  $\beta_4$ ,  $\beta_5$ .) with its Zinc ion (B) Strands with cysteine residues in bond with Zn ion. The diagram is generated as per the citation<sup>[11]</sup>

The availability of a key drug to target KSR is not available. Phytoconstituents like anthraquinone, coumarins, flavonoids, and terpenoids has wide range of pharmacological actions. The exact mode of their action has not been

completely validated for certain physiological molecular level signaling protein molecules, enzymes and receptors of therapeutic concern.

Anthraquinone derivative, damnacanthal was found to show a better binding affinity with glycogen synthase kinase-3 beta (gsk-3 $\beta$ ) through *in silico* docking studies [15].

In this study binding affinity of coumarin and anthraquinone derivatives on to the crystal structure of Cysteine rich C1 domain of kinase suppressor of Ras-1 (KSR-1) was carried out through *in silico* docking methodology.

## MATERIALS AND METHODS

The crystal structure of the investigational scaffold protein cysteine rich C1 domain of kinase suppressor of RAS (KSR) was downloaded from RCSB protein data bank [16] bearing the PDB code 1KBE. The ligands were computationally designed using Chem3DUltra8.0 [17, 18]. Ligand preparation and grid spacing set up for the search of ligands on the cavities were done with AutoDock 4.2. [19,20]. Scorings were performed with AutoDock Vina [21,], it treats docking as a stochastic global optimization of the scoring function, pre-calculating grid maps (Vina does that internally), and some other implementation tricks, such as pre-calculating the interaction between every atom type pair at every distance was done. Auto Dock Vina improves the speed and accuracy of docking with a new scoring function, efficient optimization and multithreading [22]. Pymol [23,24] viewer was used to view the overlapping of ligands at the binding site of KSR-1.

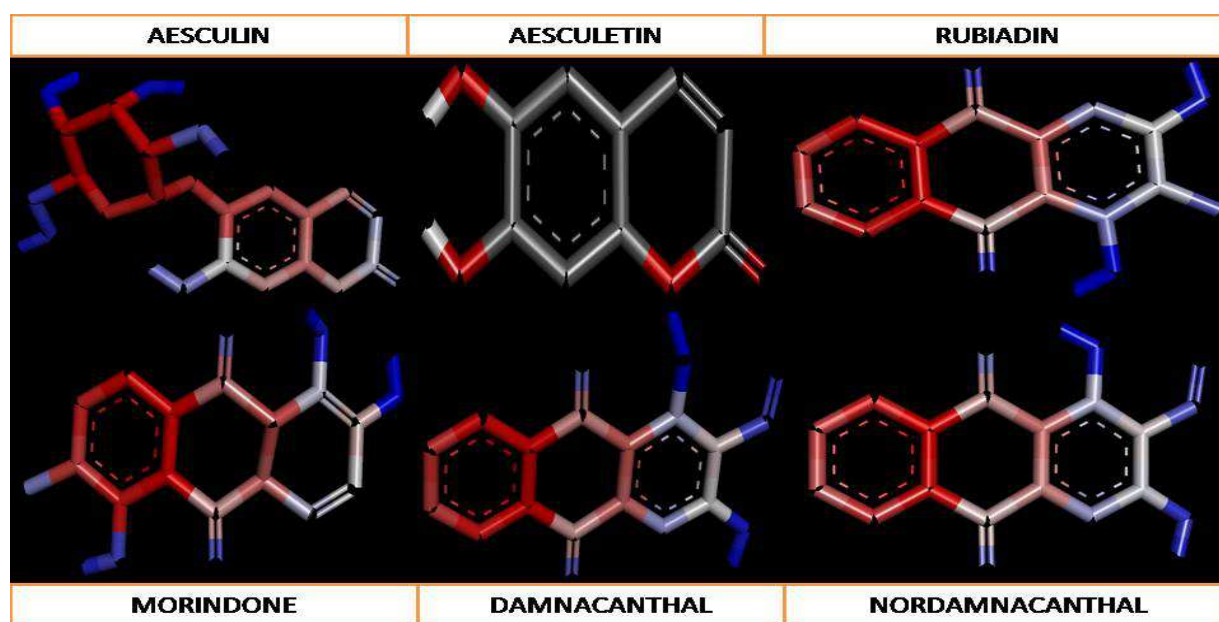


Fig 2: Image showing energy optimized ligands used for binding affinity studies

Table1: List of ligands showing their molecular formula, molar mass, hydrogen acceptors, hydrogen bond donors, Log P values, torsions.

S.No	Ligands	Molecular Formula	Molar Mass g mol <sup>-1</sup>	CAS Number	Hydrogen bond acceptors	Hydrogen bond donors	Log P	Rule of 5 No of Violations	Torsions
	Aesculin	C <sub>15</sub> H <sub>16</sub> O <sub>9</sub>	340.28	531-75-9	3	5	-1.0	0	8
	Aesculetin	C <sub>9</sub> H <sub>6</sub> O <sub>4</sub>	178.14	305-01-1	2	2	1.18	0	2
	Damnacanthal	C <sub>16</sub> H <sub>10</sub> O <sub>5</sub>	282.25	477-84-9	3	1	2.82	0	3
	Morindone	C <sub>15</sub> H <sub>10</sub> O <sub>5</sub>	270.23	478-29-5	3	3	3.82	0	3
	Nordamnacanthal	C <sub>15</sub> H <sub>8</sub> O <sub>5</sub>	268.22	3736-59-2	3	3	3.74	0	3
	Rubiadin	C <sub>15</sub> H <sub>10</sub> O <sub>4</sub>	254.23	117-02-2	2	2	3.47	0	2

**Preparation of the macromolecule (scaffold protein-KSR)**

The x-ray structure of scaffold protein containing water molecules and hetero atoms were refined using Accelrys Discovery Studio 4.0 [25]. The crystal structure was energy optimized using open Babel 2.3.2 [26, 27]. After energy minimization, scaffold protein was saved as ksr1.pdb to use it for docking studies.

**Preparation of ligands- coumarin and anthraquinone derivatives**

MOPAC (Molecular Orbital Package) is a semi-empirical quantum chemistry program based on Dewar and Thiel's NDDO approximation. MOPAC uses semi-empirical theory to calculate the electronic wave function in order to obtain molecular orbitals, the heat of formation, etc. [28]. MOPAC in Chem3D Ultra 9.0 employs AM1 (Austin Model 1) method and closed shell wave function to minimize energy to minimum RMS gradient of 0.100. AM1 belongs to the family of NDDO (Neglect of Diatomic Differential Overlap) methods. In these methods, all terms arising from the overlap of two atomic orbitals which are on different centers or atoms are set to zero. As this is not the forum for developing the ideas of Hartree-Fock theory [29], knowledge about the derivation of the Roothaan-Hall equations [30] will be assumed, and our description of the methods will start with the final equations. Properties like heat of formation, gradient norm, charges, cosmos ovation in water, electrostatic potential, molecular surfaces, spin density, hyperfine coupling constants, polarizabilities were solved and, additionally, Mulliken charges were calculated. Mulliken charges [31] provide a means of estimating partial atomic charges and are routinely used as variables in linear multiple regression QSAR procedures. 3D structures obtained after MOPAC calculations were visualized through Accelrys Discovery Studio 4.0

**Figure 2** shows the energy minimized structures of investigation ligands and these ligands were employed for docking studies.

Ligands were selected on the basis of Lipinski's rule of five. Lipinski's rule of five is to evaluate drug-likeness or to determine if a chemical compound with a certain pharmacological or biological activity has properties that would make it a likely orally active drug in humans. It explains a molecule's pharmacokinetic properties viz., absorption, distribution, metabolism and excretion. But this rule lacks to explain whether the molecule would be pharmacologically active. In the discovery setting 'the rule of 5' predicts that poor absorption or permeation is more likely when there are more than 5 H-bond donors, 10 H-bond acceptors, the molecular weight (MWT) is greater than 500 and the calculated Log P (CLogP) is greater than 5 [32,33]. Lipinski's rule of five - According to the drug likeness properties, the ligands showed zero violation of the Lipinski rule of five. **Table 1** shows their molecular weight and the Log P values for the investigating ligands.

**Docking methodology**

AutoDock 4.2 is toggled; the protein is stored as ksr.pdb. Next, ligands were converted to .pdbqt format and saved in the respective files. Then the grid icon is toggled, grid parameters were adjusted according to the area of docking. While setting up the grid, the x, y, z coordinates should be noted down, because it is needed to enter in .txt file while running up the Auto Dock Vina. The grid box was aligned as 26 X 26 X 26 dimensions on to the gorge of scaffold protein, and then it is stored as ligand.gpf. Then the files (ligand.pdbqt, ksr.pdbqt, ligand.gpf) were stored in Auto Dock Vina folder. The configuration file, it is a .txt file that has to be placed in Auto Dock Vina setup folder prior to the running the AutoDock Vina. Then the command is typed on command prompt screen as per the manual (<http://vina.scripps.edu/manual.html>) to proceed with the docking process. This involves search space volume greater than 27000 Angstrom. Then the program reads the input command followed by setting up of scoring function. Binding site analysis is carried out using random seed (818777548) then searching is performed. Finally according to the root mean square deviation the best mode of conformation with relative to the distance results were refined and log.txt file with an output of respective ligand were created. Stochastic scoring generates maximum of 9 poses with respect to their RMSD.

**Visualizing the docking results using AutoDock4.2**

The docking results were viewed using AutoDock 4.2. Toggle "analyse" tool and click the AutoDock Vina result and open respective ligand and enzyme molecules. Options displays single molecules with multiple conformations, and then select those specifications. Ligand with its binding affinity values will be displayed.

**Visualizing the docking results using PyMol viewer**

The PyMol viewer can be used to view the Vina results. This shows the overlapping of ligands in multiple conformations. Toggle the open tool bar and click down the output file of ligand and macromolecule file. It displays

the binding area of the ligand at the surface of protein. Multiple numbers of ligands can be opened on a single macromolecule to see the superimposition of the ligands.

## RESULTS

Investigating ligands interacted on to the active site gorge with maximum affinity. Lowest binding energy was shown by aesculin (-5.9kcal/mol), Morindone (5.7kcal/mol), Nordamnacanthal (-5.7kcal/mol) and Rubiadin (-5.6kcal/mol). Damnacanthal, Aesculetin was found to show a -5.2 and -4.7 kcal/mol as a free energy of binding. Followed by satisfactory results was shown by aesculetin (-4.7kcal/mol)

**Table 2: Table showing the binding affinity of the anthraquinone derivatives at the active site gorge of cysteine rich C1 domain of kinase suppressor of RAS (KSR)**

Ligands	Modes of Conformations generated at upper(9 <sup>th</sup> ) to the lowest(1st) with an RMS 0.0 Binding affinity values at each conformations, ΔG (kcal/mol)								
	1	2	3	4	5	6	7	8	9
Aesculin	-5.9	-5.8	-5.7	-5.6	-5.4	-5.3	-5.3	-5.3	-5.2
Aesculetin	-4.7	-4.5	-4.5	-4.4	-4.4	-4.4	-4.3	-4.2	-4.2
Morindone	-5.7	-5.7	-5.6	-5.6	-5.5	-5.4	-5.3	-5.2	5.1
Rubiadin	-5.6	-5.5	-5.3	-5.2	-5.2	-5.2	-5.2	-5.2	-5.0
Damnacanthal	-5.2	-5.0	-5.0	-4.9	-4.9	-4.8	-4.8	-4.8	-4.8
Nordamnacanthal	-5.7	-5.5	-5.2	-5.2	-5.1	-5.1	-5.1	-5.1	-5.0

RMSD values are calculated relative to the best mode and use only movable heavy atoms. Two variants of RMSD metrics are provided, rmsd/lb and rmsd/ub. The rmsd/ub matches each atom in one conformation with itself in the other conformation, ignoring any symmetry [34].

RMSD values for distance from the best mode of lowest binding energy possessed aesculin is 2.000 (rmsd l.b) and 3.600(rmsd u.b) for 9<sup>th</sup> mode of conformation but the best mode of conformation at rmsd (l.b and u.b) showed 0.0 as the distance from best mode. C1 domain of KSR1 was found to contain cysteine residues at Cys377, Cys370, Cys366, Cys362, Cys 359, Cys349, Cys 346.

**Table 3: Table showing the amino acids involved in hydrogen bond interaction with the investigating ligands**

S.No	Ligand	Binding affinity,ΔG (kcal/mol)	Amino Acids Involved In Hydrogen Bond Interaction	Hydrogen Bond Length(Å)
01.	Aesculin	-5.9	KSR:A:ASN368:HN 1 KSR:A:PHE336:HN 1	2.247 2.143
02.	Aesculetin	-4.7	AESCULETIN::FRA1:H1 KSR:A:HIS334:HN 1	2.246 2.128
03.	Damnacanthal	-5.2	KSR:A:THR338:HG1 DAMNACANTHAL::FRA1:H	1.992 2.182
04.	Morindone	-5.7	KSR:A:CYS377:HN 1	2.157
05.	Nor damnacanthal	-5.7	AESCULETIN::FRA1:H1	1.992
06.	Rubiadin	-5.6	KSR:A:HIS334:HN	2.127

Relating ligands binding affinity shows its specific interaction with amino acid residues at the vicinity of the receptor site. **Table 3** shows the amino acid residues involved in hydrogen bond interaction with the ligands under investigation.

## DISCUSSION

Binding affinity potential of small molecules like coumarin and anthraquinone derivatives were reported. Research on binding affinity of rare flavonoids like 2'-Hydroxygenistein was found to occupy the cysteine rich C1 domain of KSR with some limited fidelity [35]

Docking studies showed a specific interaction of investigational ligands with cysteine residues of KSR-1. **From table 3** it is evident that morindone interact with cysteine residues (Cys337) at its lowest free energy of binding (ΔG), -5.7kcal/mol

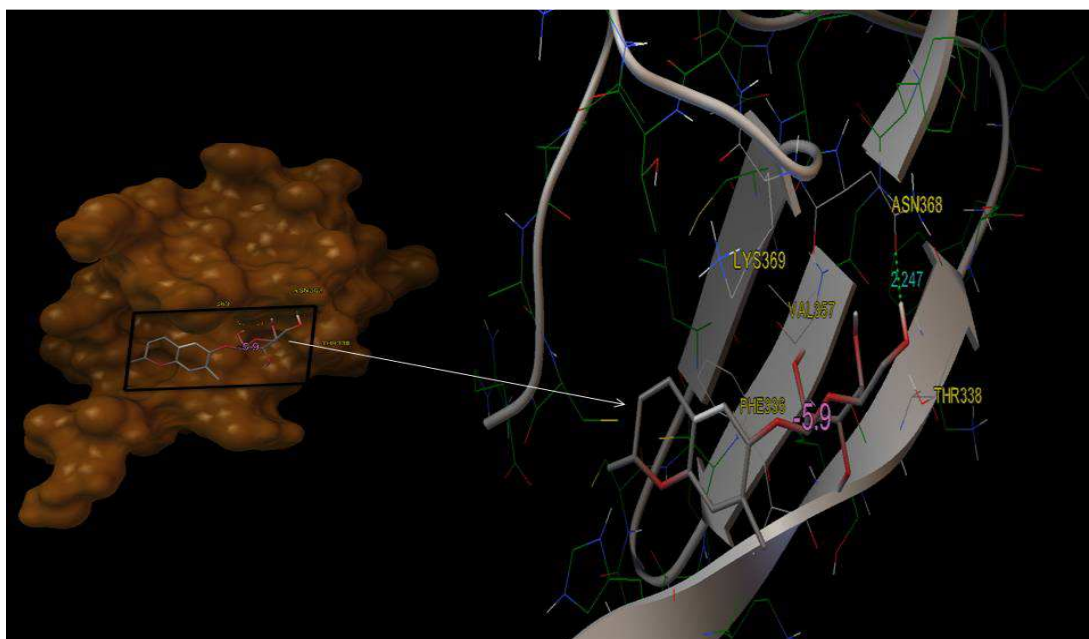


Figure 3: Surface filled image showing the binding of Aesculin at the gorge, exposed on the surface of cysteine rich C1 domain of Kinase suppressor of RAS 1 (KSR1) protein . Indication in arrows shows the ribbon image of protein emphasize its interaction with the ligand through hydrogen bonding (H bonds are shown in dotted lines).

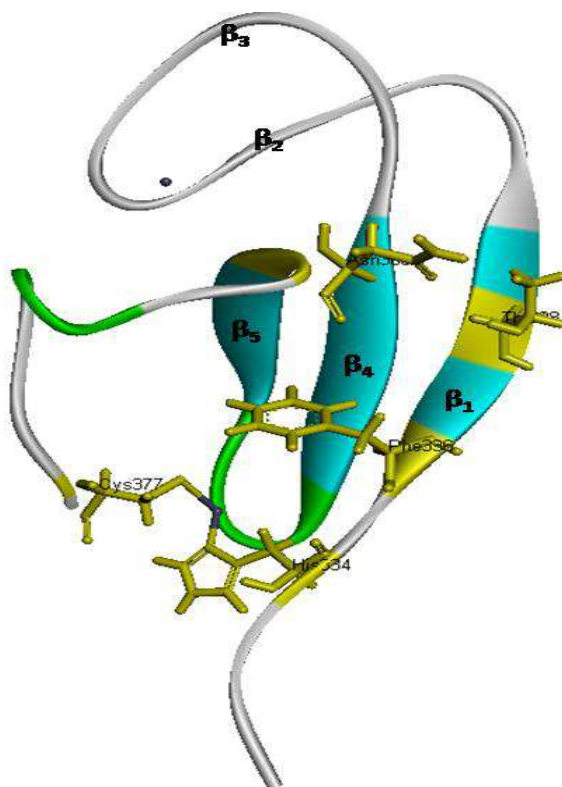
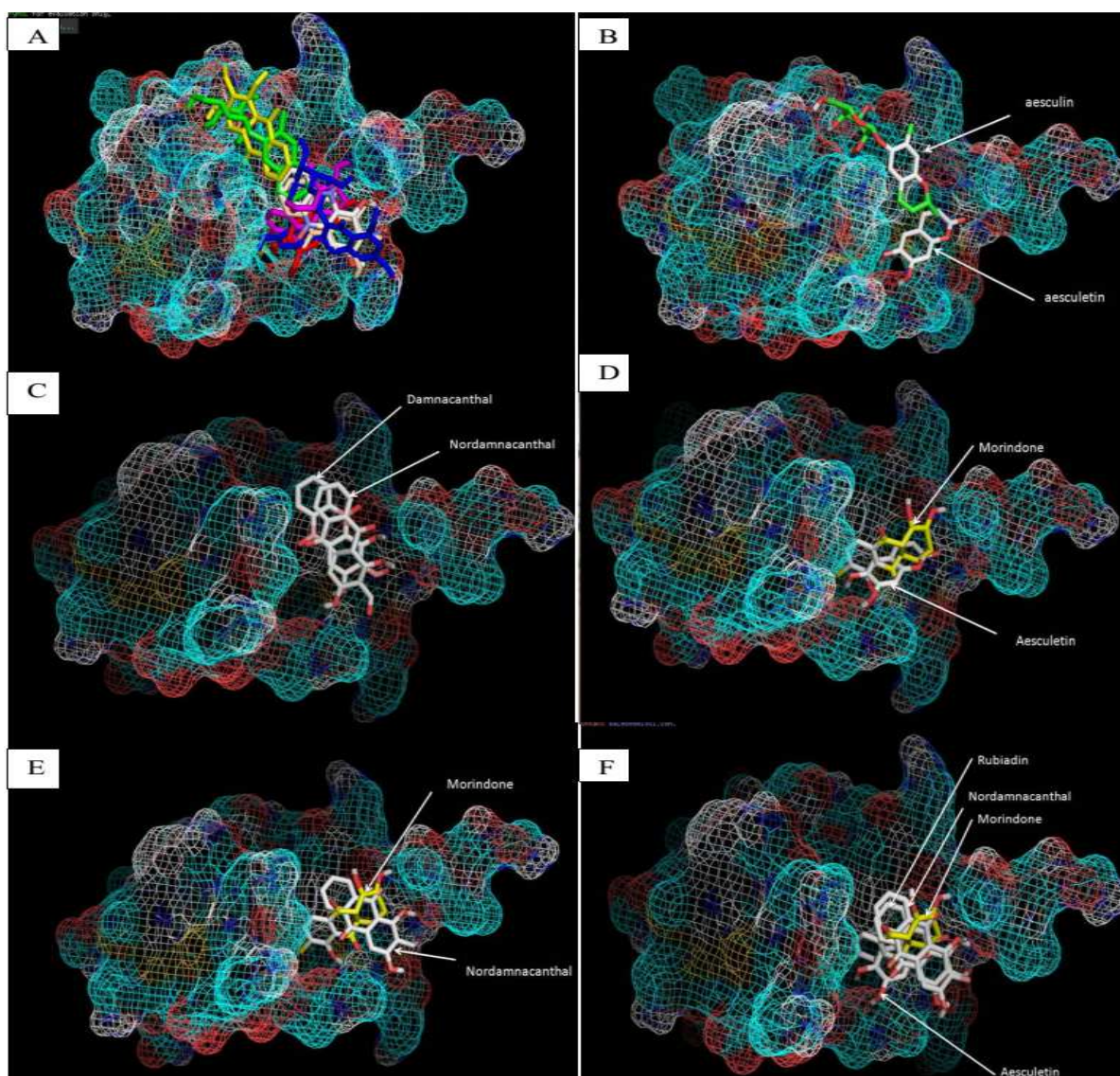


Figure 4: Image shows only the specific  $\beta$ -strand containing amino acid residues (Cys377, His334, Phe338, Thr338 and Asn368) involved in interaction with ligands (ligands are not shown in this diagram)

It has been found out some rare flavonoids like 2, 3 dehydrokieveitone was found to interact with Asn368 [35]. **Figure 3** shows aesculin interaction with Asn368 through hydrogen bonding (2.247Å), this was one of the lowest binding energy exhibited ligand under investigation. Anthraquinone and coumarin derivatives were found to interact with amino acid residues like Asn368, Phe336, His334, Thr338, Cys377 and His334.

Anthocyanidins and flavonoids also exhibited a similar mode of interactions along the beta strands,  $\beta 1$  and  $\beta 5$  [36]. The above mentioned amino acids running along beta strands  $\beta 1$  and  $\beta 5$  was found in interaction with the ligands. **Figure 4** shows the specific  $\beta$ -strand containing amino acid residues involved in interaction with ligands.

The overlapping analysis showed that the ligands with anthraquinone nucleus occupied their position with better affinity at the same vicinity (**Figure 5.A**). But there is some variation with respect to the rotatable bonds attached to the ligands.



**Figure 5:** Image showing the superimposition or overlapping of ligands investigated. A) shows overall ligands superimposition B) show the area of non overlapping binding of aesculin and aesculetin C) shows the superimposition of damnacanthal and nordamnacanthal D) shows the interfering morindone in perpendicular plane with respect to aesculetin E) similar binding affinity of morindone and nordamnacanthal but different angles of interaction F) super-imposition of rubiadin, nordamnacanthal, morindone, aesculetin.

On analyzing, overlapping of ligands at the gorge of cysteine rich C1 domain of kinase suppressor of Ras- 1 (KSR-1) scaffold protein, ligands like aesculin and damnacanthal was found to occupy the same area with a comparable affinity values. Damnacanthal and nordamnacanthal has slight difference in their structure but there was only a slight deviation in their superimposition (Fig 5.B and 5.C). Even though there are structurally different substitutions at coumarin and anthraquinone nucleus, they conserve the binding at the same gorge which shows only the affinity and not the same amino acid interaction. On visualizing the morindone and aesculetin binding affinity (Fig 5.D) there was no overlapping, instead there was a change in planar of interaction of the ligands at the active site. Aesculetin is perpendicular to the direction of morindone binding. Though the binding affinity values of Morindone and Nordamnacanthal are the same but there was a significant difference in their interaction at the active site (Fig 5.E). Not even a partial overlapping was seen but there was a differing angle of interaction. From (Fig 5.F) it is clear that Rubiadin, Nordamnacanthal, Morindone, and Aesculetin showed satisfactory superimposition.

### CONCLUSION

It is concluded that some selected coumarin and anthraquinone derivatives showed better binding affinity on the scaffolding protein-cysteine rich C1 domain of Kinase Suppressor of Ras-1(KSR-1). Targeting Kinase Suppressor of Ras-1 is of novel approach in order to shut down the molecular signaling cascade in mitogen activated protein kinase (MAPK) pathways. These scaffolding proteins can be analyzed with coumarin and anthraquinone derivatives using suitable models in *invitro* techniques to produce a lead molecule in treatment of Neoplasia.

### REFERENCES

- [1] W Kolch, *Biochem.J.*, **2000**, 35,289-305.
- [2] DA Ritt; M Zhou; TP Conrads; TD Veenstra; TD Copeland; DK Morrison, *Curr.Biol.*, **2007**, 17(2), 179-84
- [3] S Stewart; M Sundaram; Y Zhang; J Lee; M Han; KL Guan, *Mol.Cell.Biol.*, **1999**, 19, 5523– 5534.
- [4] DK Morrison; RJ Davis, *Annu.Rev.Cell.Dev.Biol.*, **2003**, 19,91–118.
- [5] G Dobrowolska; FJ Lozeman; D Li; EG Krebs, *Mol.Cell.Biochem.*, **1999**, 191, 3–12.
- [6] LA Pinna. *Int.J.Biochem.Cell.Biol.*, **1997**, 29,551–554.
- [7] M Therrien, HC Chang, NM Solomon, FD Karim, DA Wassarman GM, Rubin, *Cell.*, 83(6):879-88.
- [8] M Zhou; DA Horita; DS Waugh; RA Byrd; DK Morrison, *J.Mol.Biol.*, **2002**, 315(3), 435-46.
- [9] PE Driedger; PM Blumberg, *Proc.Natl.Acad.Sci.*, **1980**, 77, 567-571.
- [10] U Hommel; M Zurini; M Luyten, *Nat.Struct.Biol.*,**1994**, 1, 383-387.
- [11] G Zhang; MG Kazanietz; PM Blumberg; JH Hurley, *Cell.*, **1995**, 81, 917-924.
- [12] JH Hurley; AC Newton; PJ Parker; PM Blumberg; Y Nishizuka, *Protein.Sci.*, **1997**, 6, 477-480
- [13] PH Tso; Y Wang ; LY Yung; Y Tong; MM Lee; YH Wong, *Cell.Sig.*, **2013** 25(5), 1064-74.
- [14] PL Channavajhala, VR Rao, V Spaulding, LL Lin, YG Zhang, *Biochem.Biophys.Res. Commun.* **2005**, 334(4), 1214-8.
- [15] K Dhananjayan; Arunachalam S; Sivanandy P, *Elect.J.Biol.*, **2014**, 10 (1), 14-20
- [16] HM Berman; J Westbrook; Z Feng; G Gilliland; TN Bhat; H Weissig; IN Shindyalov; PE Bourne, *Nucleic.Acids.Res.*, **2000**, 28: 235-242.
- [ 17] Chem 3D Ultra 8.0, CambridgeSoft, 100 CambridgePark. Cambridge, MA 02140 USA, 1998-2001
- [18] NJ Mills, *Am. Chem. Soc.*, **2006**,128 (41), 13649–13650.
- [19] AutoDock 4.2, MGL 1.5.4, 10550 North Torrey Pines Road, CA 92037, USA, 2005-2014
- [20] GM Morris, DS Goodsell; RS Halliday; R Huey; EH William; KB Richard; AJ Olson, *J.Comp.Chem.*, **1998**, 19 (14), 1639-1662
- [21] AutoDock Vina 1.1.2, 10550 North Torrey Pines Road, CA 92037-1000, USA, 2005-2014
- [22] O Trott; AJ Olson, *J.Comp.Chem.*, **2010**,31, 455-461
- [23] PyMOL, PyMOL 1.7.2 , Schrödinger, 101 SW Main St, Suite 1300 Portland, 2009-2014
- [24]S Daniel; LG Bert, *J.Comp.Aided.Mol.Des* **2010**, 24:417–422
- [25]Discovery studio visualize 4.1, Accelrys, BIOVIA, 5005 Wateridge Vista Drive, San Diego, CA 92121, USA, 2002-2014.
- [26] NM O'Boyle, M Banck, CA James, C Morley, T Vandermeersch, GR Hutchison. *J.Chem. inform.*, **2011**, 3(33),1-14
- [27] K Dhananjayan; K Kalathil; S Arunachalam; P Sivanandy; M Parameswaran, *Orient.Pharm Exp.Med.*, **2014**, doi: 10.1007/s13596-014-0160-8
- [28] JJ Stewart, *J.Mol.Model.*, **2013**,19(1), 1-32

- [29] FF Charlotte, *Comp.Phy Comm.*, **1987**; 43(3),355–365.  
[30] CCJ Roothaan, *Rev.Mod.Phys.*, **1951**, 23,69  
[31] RS Mulliken, *J.Chem. Phys.*, **1955**; 23(10), 1833–1840  
[32] D Karthik, *J Comput Methods Mol. Des.*, **2014**, 4(2), 57-68  
[33] CA Lipinski; Lombardo F; Dominy BW; Feeney PJ; *Adv.Drug.Deliv.Rev.*, **2001**, 46(13), 3-26.  
[34] AE Cho; V Guallar; BJ Berne; R Friesner, *J. Comput. Chem.*, **2005**, 26 (9), 915-931.  
[35] K Dhananjayan; S Arunachalam, *J. Pharm. Res.*, **2014**, 8(3),423-427  
[36] D Karthik; P Majumder; S Palanisamy; K Khairunnisa; V Varsha, *Bioinformation.*, **2014**, 10(9), 580-585